

TRANSPORT PROPERTIES AND THERMAL EXPANSION OF PEROVSKITE-LIKE $\text{La}_{0.3}\text{Sr}_{0.7}\text{Fe}(\text{Al,Cr})\text{O}_{3-\delta}$ CERAMICS

A.A. Yaremchenko^a, V.V. Kharton^a, A.L. Shaula^a, M.V. Patrakeev^b, F.M.B. Marques^a

^a Department of Ceramics and Glass Engineering, CICECO, University of Aveiro, 3810-193 Aveiro, Portugal

^b Institute of Solid State Chemistry, Ural Division of RAS, 91 Pervomayskaya Str., Ekaterinburg 620219, Russia

ABSTRACT

The use of perovskite-like $(\text{Sr,L a})\text{FeO}_{3-\delta}$ as ceramic membrane materials requires extensive doping in order to increase stability and to suppress thermal and chemical induced expansion. The substitution of iron with aluminum and chromium in $\text{La}_{0.3}\text{Sr}_{0.7}\text{Fe}_{1-x-y}\text{Al}_x\text{Cr}_y\text{O}_{3-\delta}$ ($x = 0 - 0.4$; $y = 0 - 0.2$) was found to decrease total conductivity, oxygen permeability and thermal expansion coefficients. The oxygen ion transference numbers of $\text{La}_{0.3}\text{Sr}_{0.7}\text{Fe}(\text{Al,Cr})\text{O}_{3-\delta}$, determined by faradaic efficiency measurements in air, vary in the range $10^{-4} - 10^{-2}$ at 1073-1223 K, increasing with temperature. The incorporation of chromium into perovskite lattice enhances the low- $p(\text{O}_2)$ stability down to oxygen partial pressures of $2 \times 10^{-15} - 2 \times 10^{-14}$ Pa at 1173-1223 K. The solid solution formation is, however, limited to the values of $x \approx 0.30-0.35$ and $y \approx 0.07-0.08$.

Keywords: C. Ionic conductivity, C. Thermal expansion, D. Ferrites, D. Perovskites, E. Membranes

INTRODUCTION

Oxide phases with mixed oxygen-ionic and electronic conductivity are of significant interest for numerous high-temperature electrochemical applications including electrocatalytic membrane reactors for conversion of natural gas to synthesis gas.¹⁻³ One promising group of membrane materials relates to perovskite-like (La,Sr)FeO_{3-δ} showing considerable oxygen permeability under oxidizing conditions.^{4,5} These phases exhibit, however, insufficient thermodynamic and dimensional stability under large oxygen chemical potential gradients typical for membrane reactor operation.^{3,6} To some extent, the stability of (La,Sr)FeO_{3-δ} may be improved by substitution of iron with isovalent cations having stable oxidation state, such as Ga,^{6,7} or higher valence cations, such as Cr.³ The incorporation of gallium into iron sublattice was found to suppress oxygen nonstoichiometry variations and, consequently, unfavorable thermal and chemically-induced expansion.⁷ The highest level of oxygen-ionic transport in (La,Sr)(Fe,Ga)O_{3-δ} system was observed for La_{0.3}Sr_{0.7}Fe_{1-x}Ga_xO_{3-δ} series.⁵ At the same time, gallium-doped ferrites possess a number of specific disadvantages including volatilization of gallium oxide in highly-reducing atmospheres⁸ and high cost of Ga-containing raw materials. In order to explore Al substitution as an alternative to gallium and to evaluate the effect of simultaneous doping with aluminum and chromium on physicochemical and transport properties of lanthanum-strontium ferrite, the present work was focused on synthesis and characterization of La_{0.3}Sr_{0.7}Fe_{1-x-y}Al_xCr_yO_{3-δ} (x = 0-0.4, y = 0-0.2) ceramics.

EXPERIMENTAL

Powders of La_{0.3}Sr_{0.7}Fe(Al,Cr)O_{3-δ} were synthesized via glycine-nitrate process (GNP), a self-combustion technique using glycine as a fuel and nitrates of metal components as an oxidant. In the course of GNP, glycine was added into aqueous nitrate solution containing metal cations in the stoichiometric proportions. The glycine/nitrate molar ratio was double of stoichiometric calculated assuming that the only gaseous products of reaction are CO₂, N₂ and H₂O. The solution was heated on the hot plate until autoignition. Obtained foam-like powders were annealed at 1273 K for 2 h in order to remove organic residuals, grinded and calcined at 1573 K for 5 h. After ball-milling with ethanol, dense ceramic samples were pressed and sintered in air at 1723-1753 K for 5 h. Sintered samples were annealed in air at 1273 K for 3-4 h and slowly cooled in order to achieve equilibrium with air at low temperatures. The density of prepared ceramics is listed in Table 1. The characterization of ceramic materials included X-ray diffraction (XRD) analysis, scanning electron microscopy combined with energy-dispersive spectroscopy (SEM/EDS), dilatometry, and measurements of the total

conductivity (4-probe DC method) and steady-state permeation fluxes as functions of temperature and oxygen partial pressure; the experimental procedures were described elsewhere.^{5,7,9-12}

RESULTS AND DISCUSSION

XRD analysis showed formation of cubic perovskite phase for all prepared compositions; the unit cell parameters of selected materials are listed in Table 1. The ceramics of $\text{La}_{0.3}\text{Sr}_{0.7}\text{Fe}_{1-x}\text{Al}_x\text{O}_{3-\delta}$ ($x = 0.2$ and 0.3) were single-phase, whereas minor traces of SrAl_2O_4 (PDF card 74-0794) were detected in the XRD pattern of $\text{La}_{0.3}\text{Sr}_{0.7}\text{Fe}_{0.6}\text{Al}_{0.4}\text{O}_{3-\delta}$. The amount of this impurity phase, estimated from the XRD data, was less than 2%. This suggests that the solubility of aluminum cations in the iron sublattice of $\text{La}_{0.3}\text{Sr}_{0.7}\text{FeO}_{3-\delta}$ is close to 35%. The XRD patterns of $\text{La}_{0.3}\text{Sr}_{0.7}\text{Fe}_{1-y}\text{Al}_{0.3}\text{Cr}_y\text{O}_{3-\delta}$ ($y = 0.1$ and 0.2) exhibited small additional reflections assigned to $\text{Sr}_4\text{CrAl}_6\text{O}_{16}$ (PDF card 79-0237). The intensity of these secondary peaks was less than 1% with respect to the strongest perovskite reflection for $\text{La}_{0.3}\text{Sr}_{0.7}\text{Fe}_{0.6}\text{Al}_{0.3}\text{Cr}_{0.1}\text{O}_{3-\delta}$, but increases with further chromium additions. For $\text{La}_{0.3}\text{Sr}_{0.7}\text{Fe}_{0.5}\text{Al}_{0.3}\text{Cr}_{0.2}\text{O}_{3-\delta}$, extra reflections of SrCrO_4 (PDF card 35-0743) were also observed.

Table 1 lists the average thermal expansion coefficients (TEC) calculated from the dilatometric data. The drastic increase in thermal expansion at temperatures above 675-975 K is typical for perovskite-type ferrites and originates from chemically-induced expansion of the lattice due to oxygen losses on heating.⁷ The average TEC values of $\text{La}_{0.3}\text{Sr}_{0.7}\text{Fe}(\text{Al},\text{Cr})\text{O}_{3-\delta}$ ceramics vary in the range $(12.1-13.1)\times 10^{-6} \text{ K}^{-1}$ in low-temperature range and $(21.0-27.4)\times 10^{-6} \text{ K}^{-1}$ at higher temperatures, decreasing with aluminum and chromium additions.

The total conductivity of $\text{La}_{0.3}\text{Sr}_{0.7}\text{Fe}(\text{Al},\text{Cr})\text{O}_{3-\delta}$ ceramics in air (Fig.1) is predominantly electronic; the oxygen transference numbers calculated from the faradaic efficiency data are lower than 0.02 at 1223 K and decrease with reducing temperature (Table 1). The conductivity exhibits a semiconductor-type behavior at temperatures below 700-900 K, whilst further heating leads to an apparent transition to pseudometallic conduction (Fig.1). The temperature of this transition correlates with breaks on the dilatometric curves (Table 1). As for other ferrites (e.g. Ref.9), the pseudometallic behavior at high temperatures is associated, most likely, with decreasing concentration of p-type charge carriers due to increase in oxygen nonstoichiometry on heating.

Aluminum doping of $\text{La}_{0.3}\text{Sr}_{0.7}\text{Fe}(\text{Al})\text{O}_{3-\delta}$ results in decreasing conductivity (Fig.1A). Since Al^{3+} cations have stable oxidation state, their incorporation into the B sublattice of $\text{La}_{0.3}\text{Sr}_{0.7}\text{FeO}_{3-\delta}$ decreases the total concentration of B sites participating in the electronic transport, and also the absolute concentration of Fe^{4+} which represent p-type charge carriers localized on iron cations. The conductivity of $\text{La}_{0.3}\text{Sr}_{0.7}\text{Fe}_{0.7-y}\text{Al}_{0.3}\text{Cr}_y\text{O}_{3-\delta}$

ceramics is essentially independent of chromium content at temperatures above 800 K and decreases slightly with chromium additions at lower temperatures.

Fig.2 compares oxygen permeation fluxes through dense $\text{La}_{0.3}\text{Sr}_{0.7}\text{Fe}(\text{Al},\text{Cr})\text{O}_{3-\delta}$ membranes under fixed oxygen partial pressure gradient. For $\text{La}_{0.3}\text{Sr}_{0.7}\text{Fe}_{1-x}\text{Al}_x\text{O}_{3-\delta}$ ($x = 0.2$ and 0.4) ceramics, the permeation fluxes were estimated assuming negligible effect of exchange kinetics at the membrane/gas interface using Wagner equation¹:

$$j = \frac{RT}{16F^2d} \int_{p_1}^{p_2} \frac{\sigma_{\text{O}}\sigma_{\text{e}}}{\sigma_{\text{O}} + \sigma_{\text{e}}} \partial \ln p(\text{O}_2)$$

where j is permeation flux density; d is membrane thickness; p_2 and p_1 are the oxygen partial pressures at the membrane feed and permeate sides; and σ_{O} and σ_{e} are the partial oxygen-ionic and electronic conductivities, respectively, calculated from the data on total conductivity (Fig.1) and oxygen transference numbers (Table 1). The oxygen-ionic transport in $\text{La}_{0.3}\text{Sr}_{0.7}\text{Fe}(\text{Al},\text{Cr})\text{O}_{3-\delta}$ ceramics decreases with aluminum and chromium doping; also, the permeation fluxes through $\text{La}_{0.3}\text{Sr}_{0.7}\text{Fe}_{0.6}\text{Al}_{0.4}\text{O}_{3-\delta}$ membranes are 3.0-3.5 times lower than that through Ga-substituted analogue (Fig.2). Such a behavior can be attributed to lower oxygen-vacancy mobility resulting from a greater Al-O and Cr-O bond energy compared to Fe-O and Ga-O bonds, local lattice distortions near small Al^{3+} cations, which causes trapping of neighboring oxygen ions and thus decreasing the concentration of mobile ionic charge carriers, and the impurity phase segregation at the grain boundaries blocking ionic conduction in Cr-doped ceramics. The observed trends are in agreement with literature data showing that the ionic transport in $\text{La}(\text{Sr})\text{Al}(\text{Mg})\text{O}_{3-\delta}$ is substantially lower compared to LaGaO_3 -based analogues¹³, and that the vacancy diffusion coefficients in perovskite-type chromites are considerably lower than those in ferrites¹⁴. Nevertheless, the oxygen permeability of $\text{La}_{0.3}\text{Sr}_{0.7}\text{Fe}(\text{Al},\text{Cr})\text{O}_{3-\delta}$ ceramics at 1073-1223 K is higher with respect to $\text{La}_{0.8}\text{Sr}_{0.2}\text{Fe}_{0.8}\text{Co}_{0.2}\text{O}_{3-\delta}$, one representative of $(\text{La},\text{Sr})(\text{Fe},\text{Co})\text{O}_{3-\delta}$ series suggested for membrane applications.

Fig.3 presents stability limits of $\text{La}_{0.3}\text{Sr}_{0.7}\text{Fe}_{1-y}\text{Al}_{0.3}\text{Cr}_y\text{O}_{3-\delta}$ ceramics at reduced oxygen chemical potentials, as estimated from the data on $p(\text{O}_2)$ -dependencies of the total conductivity. One example of the stability boundary determination is illustrated by the inset in Fig.3, for $\text{La}_{0.3}\text{Sr}_{0.7}\text{Fe}_{0.6}\text{Al}_{0.3}\text{Cr}_{0.1}\text{O}_{3-\delta}$ at 1223 K. The oxygen partial pressure corresponding to the conductivity drop was considered as a decomposition limit at given temperature. Further reduction of $p(\text{O}_2)$ resulted in drastic degradation of the transport properties, often irreversible. The $\text{La}_{0.3}\text{Sr}_{0.7}\text{Fe}(\text{Al},\text{Cr})\text{O}_{3-\delta}$ ceramics were found to decompose at oxygen pressures, similar or even slightly lower compared to $\text{LaFeO}_{3-\delta}$, approximately 2×10^{-15} Pa at 1173 K and 2×10^{-14} Pa at 1223 K. Note that stability boundaries of other ferrite-based membrane materials, such as $\text{SrFe}(\text{Al})\text{O}_{3-\delta}$ and $\text{La}_{0.3}\text{Sr}_{0.7}\text{Fe}_{0.8}\text{Ti}_{0.2}\text{O}_{3-\delta}$,

are intermediate with respect to those of iron oxide and undoped lanthanum ferrite. The improved stability of $\text{La}_{0.3}\text{Sr}_{0.7}\text{Fe}(\text{Al},\text{Cr})\text{O}_{3-\delta}$ ceramics is related to the presence of Cr^{3+} cations, stabilizing metal-oxygen octahedra in the perovskite lattice and thus preventing decomposition.

CONCLUSIONS

The total conductivity, oxygen permeability and thermal expansion of $\text{La}_{0.3}\text{Sr}_{0.7}\text{Fe}_{1-x-y}\text{Al}_x\text{Cr}_y\text{O}_{3-\delta}$ ceramics were studied. The total conductivity in air is predominantly electronic, with the ionic contribution lower than 2% at 1223 K. The oxygen ion transference numbers decrease with reducing temperature. Although the substitution of iron with aluminum and chromium results in lower electronic and oxygen-ionic transport, thermal expansion coefficients of $\text{La}_{0.3}\text{Sr}_{0.7}\text{Fe}_{1-x-y}\text{Al}_x\text{Cr}_y\text{O}_{3-\delta}$, $(12.1-13.1)\times 10^{-6} \text{ K}^{-1}$ at 350-800 K and $(20.9-27.4)\times 10^{-6} \text{ K}^{-1}$ at 800-1300 K, also decrease with dopant content. The incorporation of chromium improves the stability under reduced oxygen chemical potentials with respect to $\text{LaFeO}_{3-\delta}$ and $\text{SrFe}(\text{Al})\text{O}_{3-\delta}$. In spite that the oxygen permeability of $\text{La}_{0.3}\text{Sr}_{0.7}\text{Fe}(\text{Al},\text{Cr})\text{O}_{3-\delta}$ is lower compared to gallium-doped analogues, co-doping with Al and Cr may constitute a promising direction of membrane materials development taking into account the high cost of gallium and volatilization of gallium oxide in reducing environments.

Acknowledgements

This work was partially supported by the FCT, Portugal (POCTI program and Project BPD/11606/2002) and the NATO Science for Peace program (project 978002).

References

1. Bouwmeester, H.J.M., Dense ceramic membranes for methane conversion. *Catal. Today*, 2003, **82**, 141-150.
2. Dyer, P.N., Richards, R.E., Russek S.L. & Taylor D.M., Ion transport membrane technology for oxygen separation and syngas production, *Solid State Ionics*, 2000, **134**, 21-33.
3. Mazanec, T.J., Electropox gas reforming. In *Ceramic Membranes I*, Eds. H.U. Anderson, A.C. Khandar & M. Liu. The Electrochemical Society, Inc., Pennington, NJ, 1997, **PV95-24**, pp.16-28.
4. ten Elshof, J.E., Bouwmeester, H.J.M. & Verweij, H., Oxygen transport through $\text{La}_{1-x}\text{Sr}_x\text{FeO}_{3-\delta}$ membranes. I. Permeation in Air/He gradients. *Solid State Ionics*, 1995, **81**, 97-109.
5. Kharton, V.V., Shaulo, A.L., Viskup, A.P., Avdeev, M., Yaremchenko, A.A., Patrakeevev, M.V., Kurbakov, A.I., Naumovich E.N. & Marques F.M.B., Perovskite-like system $(\text{Sr},\text{La})(\text{Fe},\text{Ga})\text{O}_{3-\delta}$: structure and ionic transport under oxidizing conditions. *Solid State Ionics*, 2002, **150**, 229-243.
6. Schwartz, M., White, J.H. & Sammells, A.F., Solid state oxygen anion and electron mediating membrane and catalytic membrane reactors containing them. U.S. Patent 6214757, 10 Apr. 2001.
7. Kharton, V.V., Yaremchenko, A.A., Patrakeevev, M.V., Naumovich, E.N. & Marques, F.M.B., Thermal and chemical induced expansion of $\text{La}_{0.3}\text{Sr}_{0.7}(\text{Fe},\text{Ga})\text{O}_{3-\delta}$ ceramics. *J. Europ. Ceram. Soc.*, 2003, **23**, 1417-1426.
8. Yamaji, K., Horita, T., Ishikawa, M., Sakai, N. & Yokokawa, H., Chemical stability of the $\text{La}_{0.9}\text{Sr}_{0.1}\text{Ga}_{0.8}\text{Mg}_{0.2}\text{O}_{2.85}$ electrolyte in a reducing atmosphere. *Solid State Ionics*, 1999, **121**, 217-224.
9. Patrakeevev, M.V., Mitberg, E.B., Lakhtin, A.A., Kozhevnikov, V.I., Kharton, V.V., Avdeev, M.Yu. & Marques, F.M.B., Oxygen nonstoichiometry, conductivity and Seebeck coefficient of $\text{La}_{0.3}\text{Sr}_{0.7}\text{Fe}_{1-x}\text{Ga}_x\text{O}_{2.65+\delta}$ perovskites. *J. Solid State Chem.*, 2002, **167**, 203-213.
10. Patrakeevev, M.V., Leonidov, I.A., Kozhevnikov, V.L. & Kharton, V.V., Ion-electron transport in strontium ferrites: relationships with structural features and stability. *Solid State Sciences*, in press (2004).
11. Shaulo, A.L., Kharton, V.V. & Marques, F.M.B., Phase interaction and oxygen transport in $\text{La}_{0.8}\text{Sr}_{0.2}\text{Fe}_{0.8}\text{Co}_{0.2}\text{O}_{3-\delta}$ - $(\text{La}_{0.9}\text{Sr}_{0.1})_{0.98}\text{Ga}_{0.8}\text{Mg}_{0.2}\text{O}_3$ composites. *J. Europ. Ceram. Soc.*, 2004, **24**, 2631-2639.
12. Shaulo, A.L., Vyshatko, N.P., Kharton, V.V., Tsipis, E.V., Patrakeevev, M.V., Marques, F.M.B. & Frade, J.R., Oxygen ionic transport in $\text{SrFe}_{1-y}\text{Al}_y\text{O}_{3-\delta}$ and $\text{Sr}_{1-x}\text{Ca}_x\text{Fe}_{0.5}\text{Al}_{0.5}\text{O}_{3-\delta}$ ceramics, *J. Europ. Ceram. Soc.*, in press (2003).

13. Kharton, V.V., Marques, F.M.B. & Atkinson, A., Transport properties of solid oxide electrolyte ceramics: a brief review. *Solid State Ionics*, in press (2004).
14. van Hassel, B.A., Kawada, T., Sakai, N., Yokokawa, H., Dokiya, M. & Bouwmeester, H.J.M., Oxygen permeation modeling of perovskites. *Solid State Ionics*, 1993, **66**, 295-305.
15. Charette, G.G. & Flengas, S.N., Thermodynamic properties of oxides of Fe, Ni, Pb, Cu and Mn by EMF measurements. *J. Electrochem. Soc.*, 1968, **115**, 796-804.
16. Tretyakov, Yu.D., Kaul, A.R. & Portnoy, V.K., Formation of rare earth and yttrium orthoferrites: a thermodynamic study. *High Temp. Sci.*, 1977, **9**, 61-70.

Table 1

Properties of $\text{La}_{0.3}\text{Sr}_{0.7}\text{Fe}_{1-x-y}\text{Al}_x\text{Cr}_y\text{O}_{3-\delta}$ ceramics

Composition	Density, $\text{g}\times\text{cm}^{-3}$	Unit cell parameter, nm	Average thermal expansion coefficient	
			T, K	$\alpha \times 10^6, \text{K}^{-1}$
$\text{La}_{0.3}\text{Sr}_{0.7}\text{Fe}_{0.8}\text{Al}_{0.2}\text{O}_{3-\delta}$	5.16	0.38681	350-675 / 675-1300	12.9 / 27.4
$\text{La}_{0.3}\text{Sr}_{0.7}\text{Fe}_{0.6}\text{Al}_{0.4}\text{O}_{3-\delta}$	5.02	0.38654	350-755 / 755-1300	12.1 / 23.2
$\text{La}_{0.3}\text{Sr}_{0.7}\text{Fe}_{0.6}\text{Al}_{0.3}\text{Cr}_{0.1}\text{O}_{3-\delta}$	5.39	0.38657	380-975 / 975-1350	13.1 / 22.7
$\text{La}_{0.3}\text{Sr}_{0.7}\text{Fe}_{0.5}\text{Al}_{0.3}\text{Cr}_{0.2}\text{O}_{3-\delta}$	5.14	0.38601	380-950 / 950-1350	12.4 / 21.0
Oxygen transference numbers in air				
	1223 K	1173 K	1123 K	1073 K
$\text{La}_{0.3}\text{Sr}_{0.7}\text{Fe}_{0.8}\text{Al}_{0.2}\text{O}_{3-\delta}$	4.2×10^{-3}	2.4×10^{-3}	1.4×10^{-3}	7.4×10^{-4}
$\text{La}_{0.3}\text{Sr}_{0.7}\text{Fe}_{0.6}\text{Al}_{0.4}\text{O}_{3-\delta}$	1.1×10^{-2}	6.8×10^{-3}	4.2×10^{-3}	2.5×10^{-3}
$\text{La}_{0.3}\text{Sr}_{0.7}\text{Fe}_{0.6}\text{Al}_{0.3}\text{Cr}_{0.1}\text{O}_{3-\delta}$	4.5×10^{-3}	2.5×10^{-3}	1.3×10^{-3}	6.5×10^{-4}

FIGURE CAPTIONS

Fig.1. Total conductivity of $\text{La}_{0.3}\text{Sr}_{0.7}\text{Fe}_{1-x}\text{Al}_x\text{O}_{3-\delta}$ (A) and $\text{La}_{0.3}\text{Sr}_{0.7}\text{Fe}_{1-y}\text{Al}_{0.3}\text{Cr}_y\text{O}_{3-\delta}$ (B) ceramics in air.

Fig.2. Steady-state oxygen permeation fluxes through dense $\text{La}_{0.3}\text{Sr}_{0.7}\text{Fe}(\text{Al},\text{Cr})\text{O}_{3-\delta}$ membranes under a fixed oxygen partial pressure gradient. The data on $\text{La}_{0.3}\text{Sr}_{0.7}\text{Fe}_{0.6}\text{Ga}_{0.4}\text{O}_{3-\delta}$ ⁵ and $\text{La}_{0.8}\text{Sr}_{0.2}\text{Fe}_{0.8}\text{Co}_{0.8}\text{O}_{3-\delta}$ ¹¹ are shown for comparison.

Fig.3. Low- $p(\text{O}_2)$ stability boundaries of $\text{La}_{0.3}\text{Sr}_{0.7}\text{Fe}_{1-y}\text{Al}_{0.3}\text{Cr}_y\text{O}_{3-\delta}$ ceramics estimated from the data on total conductivity. The data on Fe_xO ¹⁵, LaFeO_3 ¹⁶, $\text{SrFeO}_{3-\delta}$ ¹⁰, $\text{La}_{0.3}\text{Sr}_{0.7}\text{Fe}_{0.8}\text{Ti}_{0.2}\text{O}_{3-\delta}$ and $\text{SrFe}_{0.7}\text{Al}_{0.3}\text{O}_{3-\delta}$ ¹² are shown for comparison. Inset illustrates determination of the stability limit for $\text{La}_{0.3}\text{Sr}_{0.7}\text{Fe}_{1-y}\text{Al}_{0.3}\text{Cr}_y\text{O}_{3-\delta}$ ceramics at 1223 K.

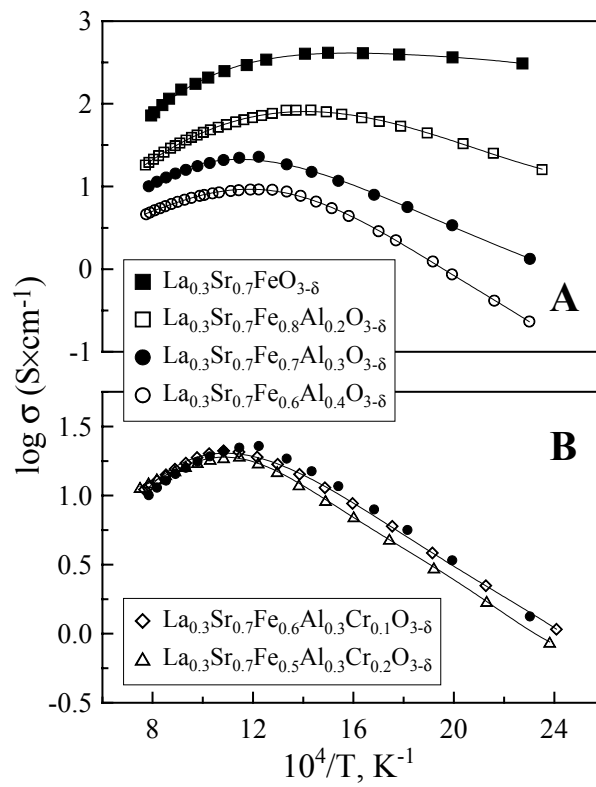


Figure 1

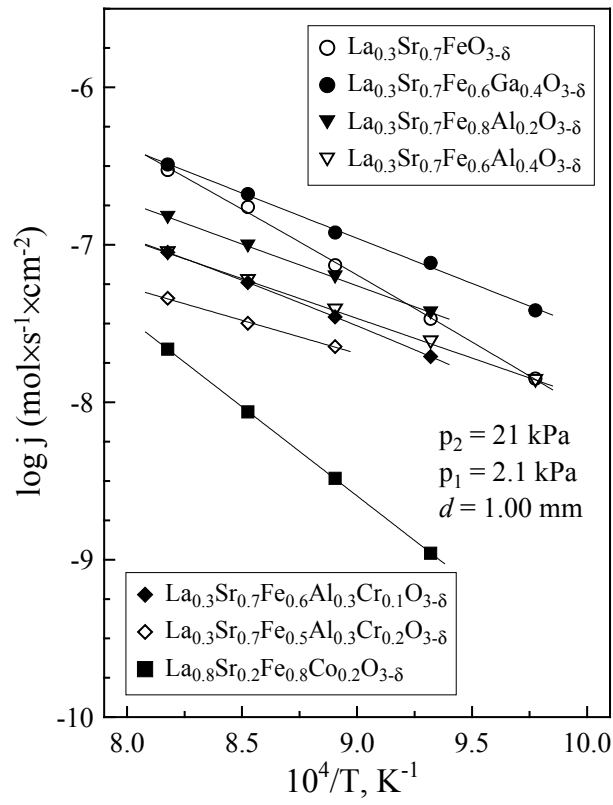


Figure 2

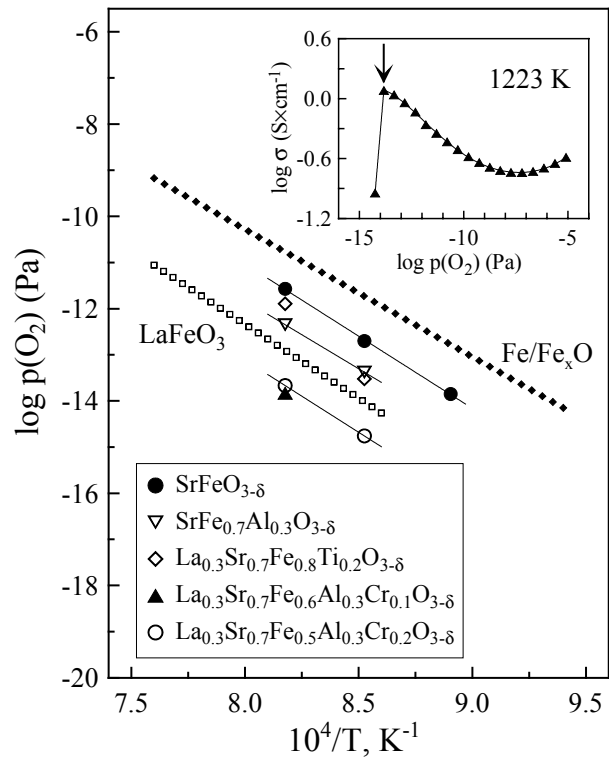


Figure 3